IUST Iran University of Science and Technology

Iranian Journal of Electrical and Electronic Engineering

Journal Homepage: ijeee.iust.ac.ir

Research Paper

Li-Ion Battery Charger Interface Circuit with Fast and Safe Charging for Portable Electronic Devices

A. Rahali*, K. El Khadiri*(C.A.), and A. Tahiri*

Abstract: In this paper, a Li-Ion Battery Charger Interface (BCI) circuit with fast and safe charging for portable electronic devices is proposed. During the charging of Li-Ion battery, current spikes due to asynchronous control signals, and temperature are factors that greatly affect battery performances and life. This circuit has the following features: prevents current spikes and also incorporates a permanent battery temperature monitoring block. The BCI uses a dual current source and generates a constant current in a large current mode of 1.5 A, further reducing charging time. The proposed BCI was designed and simulated in Cadence Virtuoso using TSMC 180 nm technology. The simulation results of the control signals show that the proposed architecture was able to eliminate the current drifts and keep the battery temperature within the normal operating range.

Keywords: Li-ion battery charger interface, Fast and safe charge, Dual current source, Trickle current mode, Large current mode, Constant voltage mode.

1 Introduction

TODDAY, portable electronic applications continue to increases. Faced with this growth, devices have become more and more energy demanding. To ensure an important autonomy, Li-ion batteries remain the most used technology to power these portable devices due to their attractive performance: high specific energy which results in batteries that are lighter, a lower rate of self-discharge (only 1 – 5% per month), immunity to the memory effect, and much better cycle life than the other batteries (>1000 cycles). Moreover, Li-ion batteries offer the advantage of a high average operating voltage of 3.6 V [1]-[4].

However, Li-ion batteries are very sensitive to overcharge, high and low temperatures and current spikes.

Iranian Journal of Electrical and Electronic Engineering, 2023.
Paper first received 21 May 2022, revised 27 Sep 2022, and accepted 01 Oct 2022.

*The authors are with Laboratory of Computer Science and Interdisciplinary Physics, ENSF, Sidi Mohamed Ben Abdellah University, Fez, Morocco.
E-mails: ahmed.rahali@usmba.ac.ma, karim.elkhadiri@usmba.ac.ma, and ahmed.tahiri@usmba.ac.ma.
Corresponding Author: K. E. Khadiri.

https://doi.org/10.22068/IJEEE.19.1.2527

Therefore, they must be charged with appropriate charging algorithms and processes to ensure safe operation of these batteries, and increase their life span. There are two processes for charging a Li-ion battery: The pulse charging process and the CC-CV (constant current – constant voltage) process [5], [6]. In the pulse charging process, a short high-peak constant current pulse is applied to the battery [5]. However, this charging process has a major drawback because the high pulses of the applied current affect the battery. The CC-CV process shown in Fig. 1 remains the widely used standard charging process for Li-ion batteries.

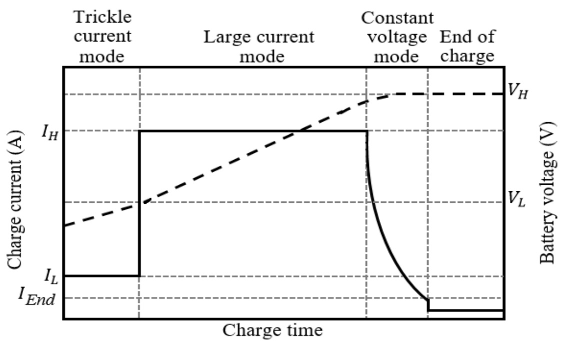

Fig. 1 CC – CV Li-ion battery charging profile.

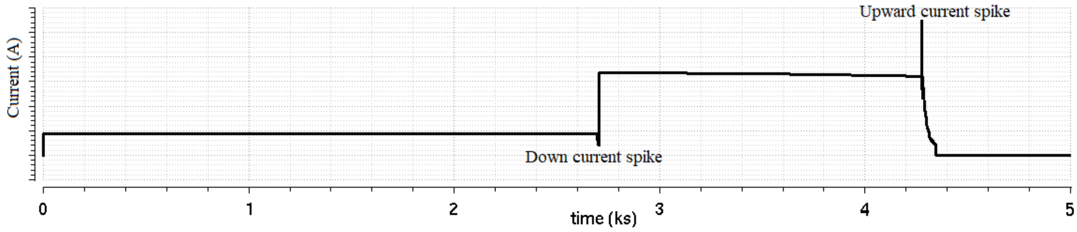

(a)

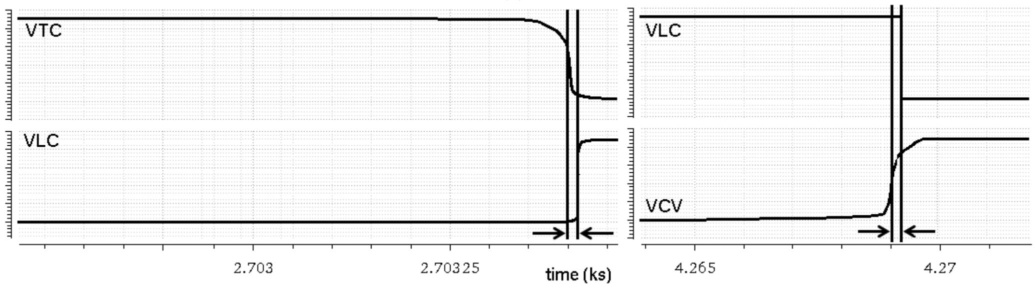

(b)

Fig. 2 Waveforms of charging current and asynchronous control signals: (a) Charging current, (b) Asynchronous control signals (V_{TC}, V_{LC}, and V_{CV}).

It consists of three charging modes: i) Trickle current mode (TC mode), ii) Large current mode (LC mode), and constant voltage mode (CV mode) described as follows:

i) If the battery voltage V_{Bat} is less than a V_L threshold, the battery is charged in TC mode and a low current is applied. This charging mode is also used to wake up a battery when it is deeply discharged.

ii) When the battery voltage reaches the V_L threshold, the battery enters the LC charging mode and the applied charging current level is maximum, the battery voltage continues to increases to the specific value V_H.

iii) Once the V_H limit is reached, the LC mode is stopped and the battery charge is switched to the CV mode. During this mode, the battery voltage is kept constant, and the charge current gradually decreases until it drops below I_{End} level ($I_{End} = \frac{1}{40} \times C$, where C is the battery capacity). At this time, the charging process is terminated and the battery is considered fully charged.

Many dedicated Li-ion battery charge ICs are designed to charge the battery in this manner [7]-[11]. In [7]-[9] , the battery charger is based on a switching power supply converter. These architectures are known for their high efficiency. But contain passive elements too huge to put in a single chip.

Linear charger architectures based on variable current source are developed [12], [13] to improve energy efficiency. However, the charge profile obtained with these architectures shows current drifts at each mode transition in the charge current Fig. 2 (a). These spikes are due to the asynchronous control signals of each mode Fig. 2 (b). Indeed, the transition from TC mode to LC mode occurs with a delay, because the V_{LC} signal changes from state “L” to state “H” after the V_{TC} signal moves to the “L” state, which causes a down current spike. Similarly, the transition to CV mode occurs earlier this time, because the signal controlling the CV mode changes from the “L” state to “H” state before the signal of LC mode is positioned at the “L” state, which leading to an upward current spike.

This problem is not the only one that has a negative impact on the battery; temperature is also a primary factor that affects not only the safety of the battery but also its performance. A Li-ion battery that charges at high temperatures begins to generate heat uncontrollably [14], [15]. On the other hand, the battery loses its capacity irreversibly when charged at low temperatures due the reduced reaction, resulting a poor charge transfer at the electrode/electrolyte interface [16], [17]. The battery is modeled in this paper by a first order Thevenin equivalent circuit described in [18]-[20].

To overcome the problem of spikes and ensure stable charge current transitions, with temperature monitoring, we introduce in this paper a charging interface using a CC-CV charging process with a dual current source. This interface incorporates a thermal protection block for the battery. The structure of this paper is organized as follows: Section 2 presents the description and analysis of the charging interface; simulation results are illustrated and discussed in section 3. Finally, section 4 is devoted to the conclusion of the whole paper.

2 Description of the Proposed Charging Interface

Fig. 3 shows the charging interface for Li-ion battery based on a dual current source. This interface uses the three-mode charging process (TC, LC and CV) described above, and includes the following blocks: charge mode selector, charge current generator, charge current controller, temperature monitoring circuit and the current sensor circuit. The dual current source is formed by two power transistors.

By comparing the battery voltage V_{Bat} with the threshold voltages V_L and V_H, the charge mode selector selects the S_1 source and/or S_2 source according to the charge mode. The charge current generator produces the currents I_{Charge} and $I_{End-charge}$ which will be compared by the charge current controller with I_{Sens} detected by the current sensor. During this time, the temperature monitoring circuit detects the normal operating range.

The battery charge will end when the I_{Sens} current drops below $I_{End-charge}$ or the battery temperature goes outside the normal operating range. This is ensured by the OR logic gate which receives on its inputs $I_{End-charge}$ and $V_{End-temp}$.

2.1 Charge Mode Selector

To avoid spikes in the charging current, the charge mode selector shown in Fig. 4 is designed so that only one control signal changes state at each transition between modes.

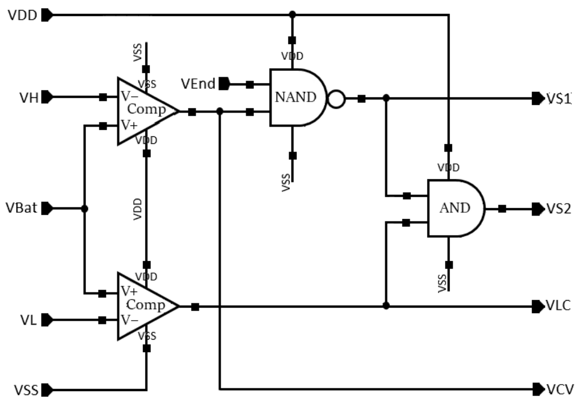

Fig. 4 Charge mode selector.

The control signals for each charging mode are generated by two comparators, which constantly compare the battery voltage V_{Bat} with the two specific values V_L and V_H. The states of these signals are described as follows:

i) When V_{Bat} is detected lower than V_L, only V_{TC} is in the "H" state.
ii) When V_{Bat} is greater than V_L and less than V_H, the V_{LC} signal switches to the "H" state and the V_{TC} signal still retains its previous state ("H").
iii) If V_{Bat} is detected greater than V_H, the V_{CV} signal changes to the "H" state. Therefore, all V_{TC}, V_{LC} and V_{CV} control signals are activated in this state.

The voltages V_{S1} and V_{S2} are generated by the NAND and AND logic gates respectively to select the current source S_1 in TC mode and both S_1 and S_2 sources in LC and CV modes. These voltages are deactivated when V_{End} is switched to the "H" state, and the current sources are deselected.

Table 1 summarizes the states of the signals generated by the charge mode selector.

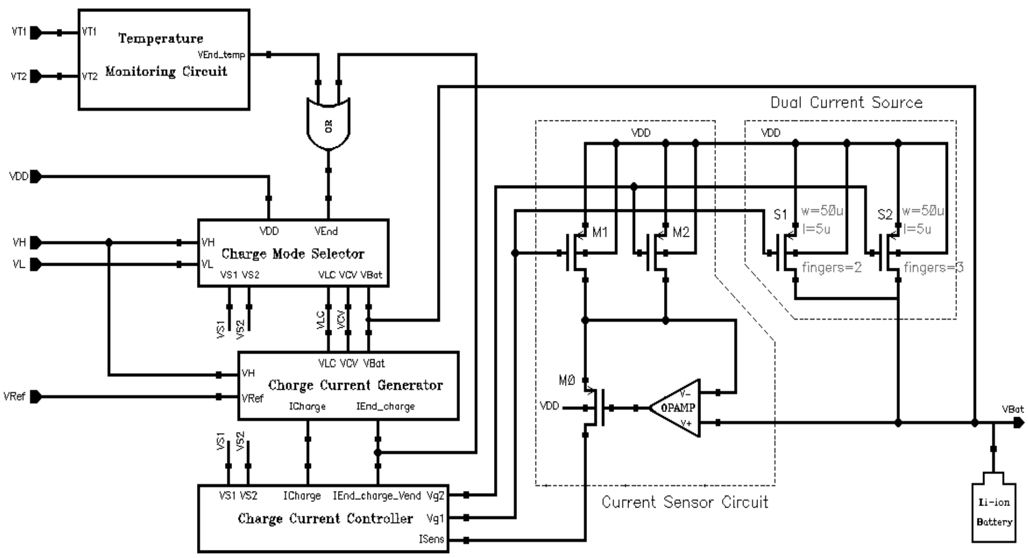

Fig. 3 Li-ion BCI with dual current source.

Table 1 Charge mode selector operation.

Charging mode	V_{TC}	V_{LC}	V_{CV}	V_{S1}	V_{S2}	V_{End}
Trickle current mode	H	L	L	H	L	L
Large current mode	H	H	L	H	H	L
Constant voltage mode	H	H	H	H	H	L
End charge	H	H	H	L	L	H

2.2 Charge Current Generator

Fig. 5 shows the charge current generator. This circuit produces the different currents for each mode in order to generate the charge current I_{Charge} and the end of charge current $I_{End-charge}$. With the operational amplifier $\mathrm{OPAMP_1}$ and M_0, the reference current I_{ref} is created and given by:

$$I_{ref} = \frac{V_{ref}}{R_0} \tag{1}$$

The currents I_{TC}, I_{LC} and $I_{End-charge}$ are generated from I_{ref} by the current mirrors (M_0:M_2), (M_0:M_1) and (M_0:M_3) respectively. While the operational amplifier $\mathrm{OPAMP_2}$ and M_8 generates the current I_{CV} when the battery voltage V_{Bat} reaches V_H. The I_{LC} and I_{CV} currents are driven via the SW_{LC} and SW_{CV} switches which are controlled by the V_{LC} and V_{CV} voltages of the charge mode selector.

(M_6:M_7), (M_9:M_{10}) and (M_{11}:M_{12}) form current mirrors and give rise to the following equations:

(M_{11}:M_{12}) and (M_6:M_7) give $I_2 = I_{CV}$ (2)

(M_9: M_{10}) give $I_1 = I_{TC} + I_{LC}$ (3)

Finally, the law of nodes at node P gives the following expression of the charge current:

$$I_{Charge} = I = I_1 - I_2 = I_{TC} + I_{LC} - I_{CV} \tag{4}$$

As consequence, the charge current in each mode is given by:

a) In TC mode, as the V_{LC} and V_{CV} control signals are deactivated, the I_{LC} and I_{CV} are zero and the charge current reduces to I_{TC}.
b) In LC mode, V_{CV} is deactivated resulting in I_{CV} being zero and $I_{Charge} = I_{TC} + I_{LC}$.
c) In CV mode, V_{CV} is activated and the I_{CV} current increases significantly, which decreases the charge current I_{Charge} to value close 0.

2.3 Charge Current Controller

Fig. 6 shows the charge current controller. This circuit receives I_{Charge} and $I_{End-charge}$ currents from the charge current generator to compare them with the detected current I_{Sens} from the current sensor and provides the different gate voltages V_{g1}, V_{g2} to the dual current source for each charge mode.

The transconductance amplifier OTA and (M_4, M_6) compare I_{Charge} with I_{Sens}. Depending on the comparison result, the voltage V_S of the pair of inverters (M_0, M_2) and (M_1, M_3) varies in each mode. Moreover, the V_{S1} and V_{S2} voltages of the charge mode selector control this pair of inverters. Finally, the voltages V_{g1} and V_{g2} are created in order to drive the power PMOSs (dual current source).

At the same time, M_5 and M_6 compare I_{Sens} with $I_{End-charge}$ and activate the $V_{End-charge}$ voltage when I_{Sens} is detected less than $I_{End-charge}$. In this case V_{S1} and V_{S2} are set to the low state (Table 1) consequently, the current sources S_1 and S_2 are deselected.

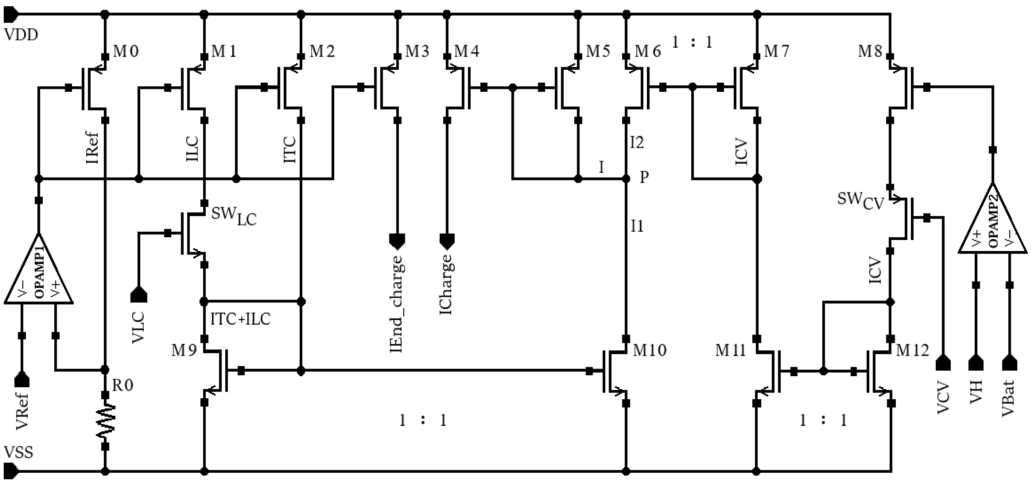

Fig. 5. Charge current generator.

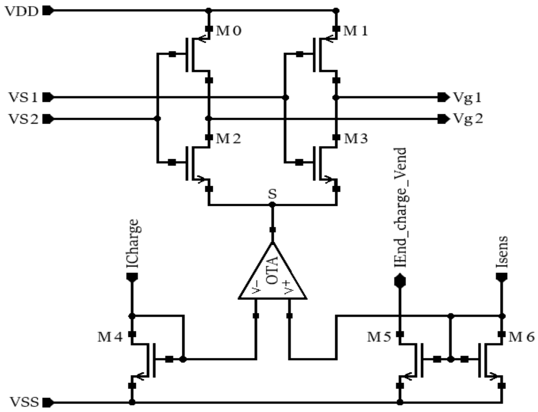

Fig. 6 Charge current controller.

2.4 Temperature Monitoring Circuit

To monitor the temperature of the battery during the charging process, the monitoring circuit shown in Fig. 7 is designed to stop charging when the battery temperature goes outside the normal operating range [0 °C-45 °C]. This circuit consists of a Proportional to Absolute Temperature (PTAT), two comparators and an inequality detector.

Fig. 8 shows the PTAT generator circuit used. The principle of this circuit is similar to that of a previous work [21], and consists of generating a voltage V_{PTAT} proportional to the temperature. The comparators Comp_1 and Comp_2 are used to compare the V_{PTAT} voltage with the reference voltages V_{T1} and V_{T2} which correspond to the limit values 0 °C and 45 °C. Depending on the result of this comparison, V_1 and V_2 can assume the states "H" or "L".

The inequality detector circuit detects the safe operating range. When the battery temperature is outside this range, this circuit activates $V_{End-temp}$ to suspend the charging process. If the battery temperature returns to the normal operating range, $V_{End-temp}$ is deactivated and the process resumes from where it stoped. The states of the V_1, V_2 and $V_{End-temp}$ signals are presented in Table 2.

Table 2 Temperature monitoring circuit operation.

Temperature conditions	V_1	V_2	$V_{End-temp}$
Cold temperature range	L	L	H
Normal temperature range [0 °C – 45 °C]	H	L	L
Hot temperature range	H	H	H

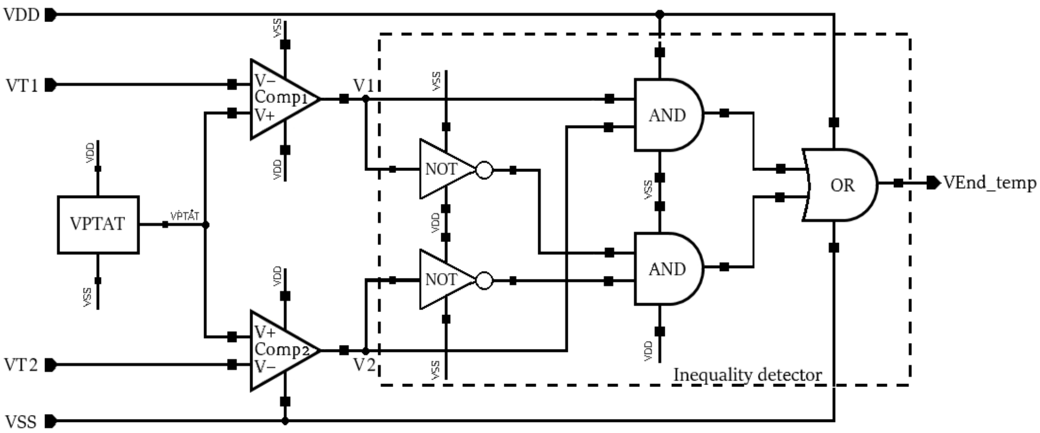

Fig. 7 Temperature monitoring circuit.

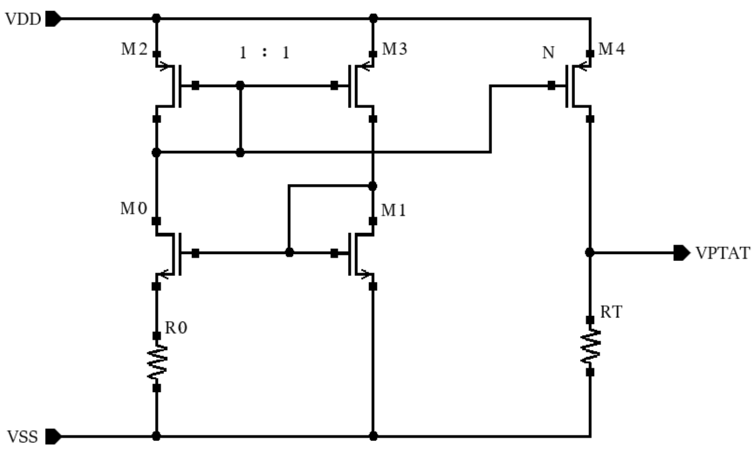

Fig. 8 PTAT generator circuit.

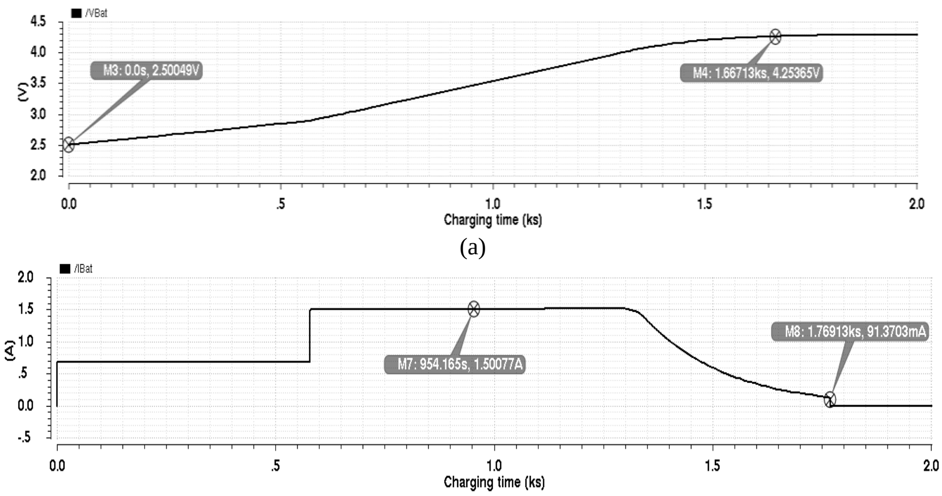

(b)

Fig. 9 Simulated charging profile of the BCI: (a). Battery voltage (V_{Bat}), (b). Battery current (I_{Bat}).

2.5 Current Sensor Circuit

As shown in Fig. 3, the current sensor circuit consists of two transistors M_1, M_2 and an operational amplifier. M_1 and M_2 detect the currents of power PMOSs (S_1, S_2) and generate the I_{Sens} current which is compared by charge current controller with I_{Charge} and $I_{End-charge}$. The operational amplifier is used to equalize the voltages V_{ds} of M_1 and M_2 with the voltage of the current source. Consequently, the generated I_{Sens} is proportional to the charge current of the battery I_{Bat}.

3 Simulation Results and Discussion

The proposed Li-ion BCI is designed and simulated in Cadence Virtuoso using TSMC 180 nm technology. The threshold voltages V_L and V_H are chosen to be 2.9 V and 4.2 V respectively.

Figures 9 (a) and 9 (b) show the variations of V_{Bat} and I_{Bat} at the temperature 27 °C. Fig. 9 (a) shows that the voltage V_{Bat} varies from 2.5 V to 4.2 V. Fig. 9(b) shows that I_{Bat} takes a low current when V_{Bat} is below 2.9 V and reaches a maximum of 1.5 A when V_{Bat} is between 2.9 V and 4.2 V. The battery charge ends after 29 min, which qualifies this charging interface as fast.

The waveforms of the control signals V_{LC}, V_{CV} and the selection voltages V_{S1} and V_{S2} are shown in Fig. 10. Fig. 10 (a) shows that the TC/LC and LC/CV transitions occur with only one signal changing state, thus avoiding spikes in the I_{Bat} current. As shown in Fig. 10 (b), only the source S_1 which is selected to charge the battery during the TC phase and in the LC and CV phases both sources S_1 and S_2 are selected. These sources are deselected when the V_{End} voltage is activated.

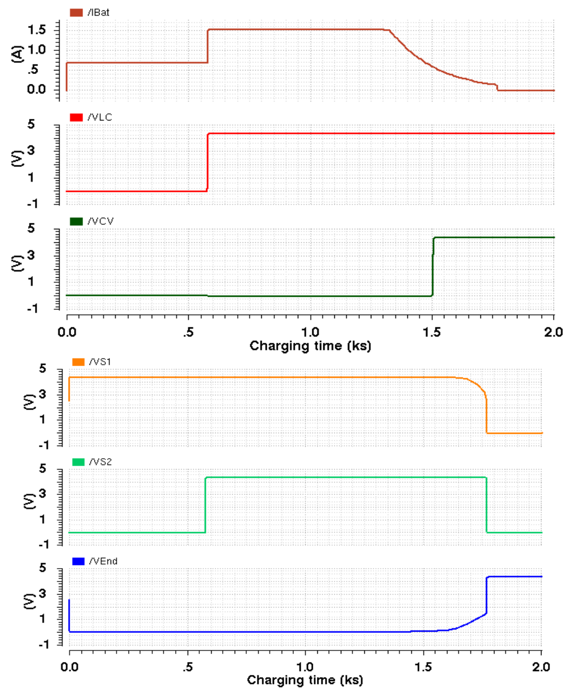

(b).

Fig. 10 Waveforms of the control and selection signals. (a) Control signals V_{LC}, V_{CV} and battery current, (b) Selection voltage V_{S1}, V_{S2} and V_{End}

Fig. 11 shows the detection of the temperature range [0 °C- 45 °C] that corresponds to the Li-ion battery's safe charging range. The $V_{End-temp}$ voltage is activated outside this range to suspend the charging process. $V_{End-temp}$ is deactivated as soon as the temperature returns to the normal operating range to restart the battery charge. The performance of the proposed BCI and a comparison with previous work are summarized in Table 3, which includes the results of four Li-ion battery charger ICs designs reported in recent papers.

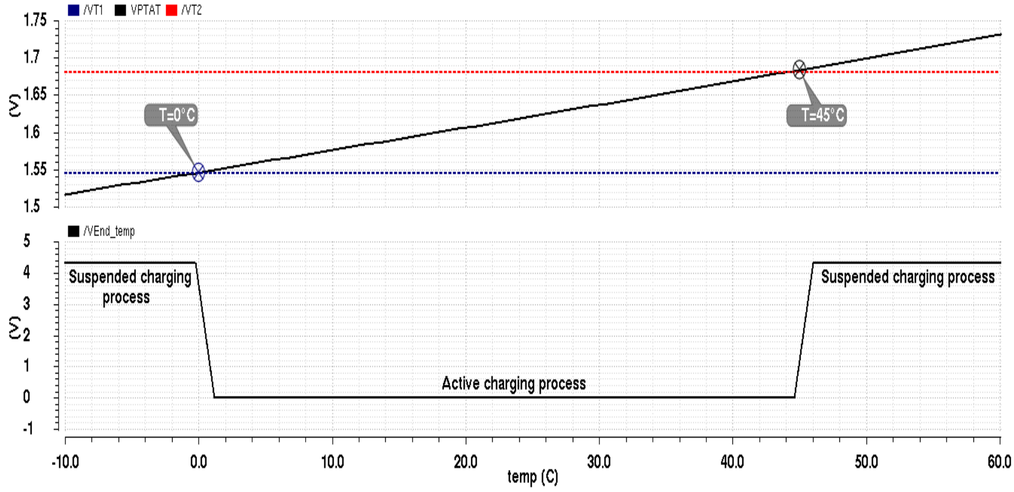

Fig. 11 Detection of safe charging temperature range and $V_{End-temp}$ voltage waveform.

Table 3 Performance summary and comparison with other Li-ion battery charger IC's.

Ref.	[10]* 2015	[22] 2017	[23] 2019	[9] 2021	This work
Process (μm)	0.18 CMOS	0.13 BCD	0.5 CMOS	0.18 CMOS	0.18 CMOS
Charger type	Adaptive LDO	LDO	Switching	Switching	LDO
Maximum Input Voltage (V)	5	5	10	4.5	4.3
Output Voltage range (V)	2.5 – 4.2	3 – 4.3	2.5 – 4.2	2.7 – 4.2	2.5 – 4.2
Maximum Charging Current (A)	448 m	495 m	1.5	1.7	1.5
Peak Efficiency (%)	87 at 4.8 V 84 at 5 V	83.9	87.4 (CC) 88.6 (CV)	97	90.6
Temperature monitoring function	Yes	No	No	No	Yes

* High temperature monitoring only

Compared to the LDO-based architectures presented in [10] and [22], only the interface proposed in this work achieved a maximum current of 1.5 A with a high efficiency of 90.6%.

The switching chargers presented in [9] and [23] can guarantee higher efficiency, but without any battery temperature monitoring.

4 Conclusion

In conclusion, a Li-Ion BCI circuit with fast and safe charging for portable electronic devices has been successfully designed in 180 nm CMOS technology. Circuit design, simulation and analysis are all included in this study. This BCI uses a 4.3 V supply and provides an output voltage of 2.5 V to 4.2 V. The simulation results show the robustness of this charging interface with respect to current spikes, which allowed us to increase the charge current in LC mode up to 1.5 A to reduce the charge time while keeping the battery temperature within the desirable operating range and thus ensuring a long life for the Li-ion battery. The chip possesses super characteristics suitable for portable electronic devices.

Intellectual Property

The authors confirm that they have given due consideration to the protection of intellectual property associated with this work and that there are no impediments to publication, including the timing to publication, with respect to intellectual property.

Funding

No funding was received for this work.

CRediT Authorship Contribution Statement

A.Rahali: dea & Conceptualization, Research & Investigation, Methodology, Revise & Editing. **K. E. khadiri**: Idea & Conceptualization,Software and Simulation, Data Curation, Original Draft Preparation, Revise & Editing, Methodology. **A. Tahiri:** Supervision, Verification, Revise & Editing.

Declaration of Competing Interest

The authors hereby confirm that the submitted manuscript is an original work and has not been published so far, is not under consideration for publication by any other journal and will not be submitted to any other journal until the decision will be made by this journal. All authors have approved the manuscript and agree with its submission to

"Iranian Journal of Electrical and Electronic Engineering".

References

[1] D. Deng, "Li-ion batteries: basics, progress, and challenges," *Energy Science & Engineering.*, Vol. 3, No. 5, pp. 385-418, 2015.

[2] D. Linden, and T. B. Reddy, "Lithium-ion batteries," in Handbook of batteies, *Mc Graw-Hill, 3th ed. New York*, USA, ch 35, pp 35.2, 2002.

[3] C. Capasso, O. Veneri, "Experimental analysis on the performance of lithium based batteries for road full electric and hybrid vehicles," *Applied Energy*, Vol. 136, pp. 921-930, 2014.

[4] B. Diouf, R. Pode, "Potential of lithium-ion batteries in renewable energy," *Renewable Energy*, Vol. 76, pp. 375-380, 2015.

[5] B. Tar, and A. Fayed, "An overview of fundamentals of battery, " *in Proc. IEEE 59th Int. Midwest Symp Circuits Syst. (MWSCAS)*, pp. 1-4, 2016.

[6] S. S. Zhang, K. Xu, and T. R. Jow, "Study of the charging process of a LiCoO2-based Li-ion battery," *Journal of Power Sources*, Vol. 160, No. 2, pp. 1349-1354, 2006.

[7] C. C. Su, Y. W. Liu, and C. C. Hung, "A dual-input high-efficiency Li-ion battery charger with current-mode smooth transition and ripple reduction circuits," *IEEE 60th International Midwest Symposium on Circuits and Systems (MWSCAS)*, pp. 468-471, 2017.

[8] M. G. Jeang, S. H. Kim, and C. Yoo, "Switching battery charger integrated circuit for mobile devices in a 130-nm BCDMOS process," *IEEE Transactions on Power Electronics*, Vol. 31, No. 11, pp. 7943-7952, 2016.

[9] M. E. Alaoui, F. Farah, K. El Khadiri, A. Tahiri, R. El Alami, H. Qjidaa, "A high efficiency and high speed charge of Li-ion battery charger interface using switching-based technique in 180nm CMOS technology," *International Journal of Power Electronics and Drive Systems*, Vol. 12, No. 1, pp. 374-384, 2021.

[10] Y. Ziadi and H. Qjidaa, "A high efficiency Li-ion battery LDO-bsed charger for portable application," *Active and Passive Electronic Components*, Vol. 2015, 2015.

[11] H. M. Nguyen, L. D. Pham, and T. Hoang, "A novel Li-ion battery charger using multi-mode LDO configuration based on 350nm HV-CMOS," *Analog Integrated Circuits and Signal Processing*, Vol. 88, No. 3, pp. 505-516, 2016.

[12] J. J. Chen, F. C. Yang, C. C. Lai, Y. S. Hwang, and R. G. Lee, "A high efficiency multimode Li-ion battery charger with variable current source and controlling previous-stage supply voltage," *IEEE Transactions on Industrial Electronics*, Vol. 56, No. 7, pp. 2469-2478, 2009.

[13] H. Y. Yang, T. H. Wu, J. J. Chen, Y. S. Hwang, and C. C. Yu, "An omnipotent Li-ion battery charger with multimode controlled techniques," *2013 IEEE 10th International Conference on Power Electronics and Drive Systems*, pp. 531-534, 2013.

[14] G. Liu, M. Ouyang, L. Lu, J. Li, and X. Han, "Analysis of the heat generation of lithium-ion battery during charging and discharging considering different influencing factors," *Journal of Thermal Analysis and Calorimetry*, Vol. 116, No. 2, pp. 1001-1010, 2014.

[15] S. Ma, M. Jiang, P. Tao, C. Song, J. Wu, J. Wang, T. Deng, and W. Shang, "Temperature effect and thermal impact in lithium-ion batteries: A review," *Progress in Natural Science: Materials International*, Vol. 28, No. 6, pp. 653-666, 2018.

[16] T. Bandhauer, S. Garimella, T. Fuller, "A critical review of thermal issues in lithium-ion batteries," *Journal of The Electrochemical Society*, Vol. 158, No. 3, pp. R1–R25, 2011.

[17] C. Vidal, O. Gross, R. Gu, P. Kollmeyer, and A. Emadi, "xEV Li-ion battery low-temperature effects-review," *IEEE Transactions on Vehicular Technology*, Vol. 68, No. 5, pp. 4560-4572, 2019.

[18] X. Zhang, W. Zhang, and G. Lei, "A review of Li-ion battery equivalent circuit models," *Transactions on Electrical and Electronic Materials.*, Vol. 17, No. 6, pp. 311-316, 2016.

[19] X. Gong, R. Xiong, and C. C. Mi, "Study of the characteristics of battery packs in electric vehicles with parallel-connected lithium-ion battery cells," *Applied Power Electronics Conference and Exposition (APEC)*, pp. 1872-1879, 2014.

[20] S. M. Mousavi G. , M. Nikdel, "Various battery models for various simulation studies and applications," *Renewable and Sustainable Energy Reviews*, Vol. 32, pp. 477-485, 2014.

[21] A. Rahali, M. Ouremchi, A. Elboutahiri, K. El Khadiri, A. Tahiri, H. Qjidaa, "Design of a temperature sensor with 0°C to 120°C sensing range for Li-ion battery charger in 180nm CMOS technology," *7th Mediteranean Congress of Telecommunications (CMT)*, 2019.

[22] K. Chung, S. K. Hong, and O. K. Kwon, "A fast and compact charger for an Li-ion battery using successive built-in resistance detection," *IEEE Transactions on Circuits and Systems II: Express Briefs*, Vol. 64, No. 2, pp. 161-165, 2017.

[23] C. C. Wang, and G. X. Liu, "A 1.5A 88.6% Li-ion battery charger design using pulse swallow technique in light load," *in Conf. Proc. of 2019 IEEE Int. Symposium on Circuits and Systems (ISCAS)*, 2019.

A.Rahali received his Master degree in Microelectronics from Faculty of Sciences Dhar El Mahraz, Fez, Morocco, in 2018. He is now a PhD candidate in Laboratory of Computer Science and Interdisciplinary Physics (LIPI), Superior Normal School, ENS-FEZ, Morocco. His research interests include renewable energy, CMOS mixed-mode integrated circuit design, development of integrated circuits for BMS, Li-ion battery charger and power management.

K. El khadiri was born in Fez, Morocco in 1978. He received M.S. and Ph.D. degrees in Faculty of Sciences from Sidi Mohammed Ben Abdellah University in 2011 and 2017, respectively. Since 2012, he served as a Research Scientist at Faculty of science in the University of Sidi Mohammed Ben Abdellah, Fez, Morocco and guest researcher at LIMA laboratory in UQO Canada. His current interests include switch mode audio amplifier, CMOS mixed-mode integrated circuit design, design techniques for RFID, RF front-ends for passive tags, Li-Ion battery charger and power management.

A. Tahiri received the M. Sc. degree in LESSI from Department of Physics, Sidi Mohammed Ben Abdellah University, Morocco in 2003, received the Ph. D. degree in physics and environment from the University Sidi Mohamed Ben Abdellah, Faculty of Science, Morocco in 2005. He completed his doctoral studies in didactics of science in the University of Sherbrooke in Canada in 2009. He is now a professor in Superior Normal School, Morocco. His research interests include image processing, didactics of scientific disciplines, renewable energy, switch mode audio amplifier, CMOS mixed mode integrated circuit design, design techniques for RFID, Li-Ion battery charger and power management.